Galactic diffuse gamma-ray emission at TeV energy

A. Neronov, D. Semikoz

A&A 633, A94 (2020)
https://doi.org/10.1051/0004-6361/201936368

Astronomy & Astrophysics

Galactic diffuse gamma-ray emission at TeV energy

A. Neronov[1,2] and D. Semikoz[1]

[1] APC, University of Paris, CNRS/IN2P3, CEA/IRFU, 10 rue Alice Domon et Leonie Duquet, Paris, France
[2] Astronomy Department, University of Geneva, Ch. d'Ecogia 16, 1290 Versoix, Switzerland
e-mail: andrii.neronov@unige.ch

Received 24 July 2019 / Accepted 30 November 2019

ABSTRACT

Context. Measuring the diffuse Galactic γ-ray flux in the TeV range is difficult for ground-based γ-ray telescopes because of the residual cosmic-ray background, which is higher than the γ-ray flux by several orders of magnitude. Its detection is also challenging for space-based telescopes because of low signal statistics.
Aims. We characterise the diffuse TeV flux from the Galaxy using decade-long exposures of the *Fermi* Large Area Telescope.
Methods. Considering that the level of diffuse Galactic emission in the TeV band approaches the level of residual cosmic-ray background, we estimated the level of residual cosmic-ray background in the SOURCEVETO event selection and verified that the TeV diffuse Galactic emission flux is well above the residual cosmic-ray background up to high Galactic latitude regions.
Results. We study spectral and imaging properties of the diffuse TeV signal from the Galactic plane. We find much stronger emission from the inner Galactic plane than in previous HESS telescope estimates (lower bound). We also find a significant difference in the measurement of the Galactic longitude and latitude profiles of the signal measured by *Fermi* and HESS. These discrepancies are presumably explained by the fact that regions of background estimate in HESS have non-negligible γ-ray flux. Comparing *Fermi* measurements with those of ARGO-YBJ, we find better agreement, with the notable exception of the Cygnus region, where we find much higher flux (by a factor 1.5). We also measure the TeV diffuse emission spectrum up to high Galactic latitude and show that the spectra of different regions of the sky have spectral slopes consistent with $\Gamma = 2.34 \pm 0.04$, which is harder than the slope of the locally observed spectrum of cosmic rays with energies 10–100 TeV, which produce TeV diffuse emission on their way through the interstellar medium. We discuss the possible origin of the hard slope of the TeV diffuse emission.
Conclusions. *Fermi*/LAT provides reliable measurements of the diffuse Galactic emission spectrum in the TeV range, which are almost background free at low Galactic latitudes. The diffuse flux becomes comparable to the residual cosmic-ray background at Galactic latitudes $|b| > 50°$. Its measurement in these regions might suffer from systematic uncertainty stemming from the uncertainty of our phenomenological model of the residual cosmic-ray background in the Pass 8 *Fermi*/LAT data.

Key words. gamma rays: diffuse background – gamma rays: ISM – radiation mechanisms: non-thermal

1. Introduction

After ten years of operations, *Fermi* Large Area Telescope (LAT; Atwood et al. 2009) has accumulated statistics of the γ-ray signal from the sky sufficient for exploration of diffuse sky emission in the TeV band, which overlaps the energy band that is accessible to the ground-based γ-ray telescopes. Although the effective collection area of the LAT is orders of magnitude smaller than that of the ground-based γ-ray telescopes, its sensitivity for the diffuse sky signal is comparable to or better than that of the ground-based telescopes because the suppression of the charged cosmic-ray background on top of which the γ-ray signal is detected is orders of magnitude better.

Detection of diffuse γ-ray flux in the multi-TeV range has been reported by High Energy Stereoscopic System (HESS; Abramowski et al. 2014), Milagro (Abdo et al. 2008), and the Astrophysical Radiation with Ground-based Observatory at YangBaJing (ARGO-YBJ; Bartoli 2015) collaborations. Ground-based telescopes are better suited for measuring signals from isolated point sources, for which the level of cosmic-ray background can be directly estimated from a comparison of the signal from the source direction with the signal from adjacent sky regions around the source, or in the same declination strip on the sky. In contrast, measuring diffuse emission is challenging because it is impossible to find an adjacent signal-free region on the sky from a priori considerations. In this respect, even though the statistics of the *Fermi*/LAT signal is much lower than that of the ground-based telescopes, LAT measurements are complementary to the ground-based measurements and could be used for improvement of the ground-based measurements, for example, through identification of optimal regions for a background estimate.

The diffuse emission in the TeV energy range comes almost exclusively from cosmic-ray interactions in the interstellar medium because the extragalactic γ-ray flux is strongly suppressed by the pair production on extragalactic background light. The inverse Compton flux from cosmic-ray electrons in the interstellar medium is suppressed by the softening of the electron spectrum in the multi-TeV range and by the onset of Klein-Nishina suppression of the Compton-scattering cross-section. Thus, the dominant component of the multi-TeV diffuse emission is provided by interactions of cosmic-ray protons and nuclei with energies in the 10–100 TeV range.

In this respect, the study of diffuse γ-ray flux in the multi-TeV range provides a straightforward probe of the distribution of cosmic rays with energies above 10 TeV in the local interstellar medium and in the large-scale cosmic-ray halo of the Milky Way (their interactions produce diffuse emission

at high Galactic latitude) and across the Milky Way disc (generating the bulk of emission at low Galactic latitude). Different models of the cosmic-ray population in the Galactic disc were considered. Lower energy *Fermi*/LAT data indicate that the spectrum of cosmic rays in the inner Galactic disc is harder than that in the local Galaxy (with the slope close to $dN/dE \propto E^{-\Gamma}$ with $\Gamma \simeq 2.4 \ldots 2.5$, rather than $\Gamma > 2.7$ measured locally) (Neronov & Malyshev 2015; Yang et al. 2016; Acero et al. 2016). This could be explained either by a model in which the "universal" slope of the cosmic-ray spectrum determined by the balance of injection by shock acceleration produces an injection spectrum with a slope $\Gamma_0 \simeq 2$, followed by the escape through the magnetic field, with a Kolmogorov turbulence spectrum resulting in the softening of the spectrum down to $\Gamma \simeq \Gamma_0 + \delta$, $\delta = 1/3$ (Neronov & Malyshev 2015), or by a model in which the energy dependence of the cosmic-ray diffusion coefficient δ changes with the distance from the Galactic center (Gaggero et al. 2015). Model predictions of the universal and Galactocentric-distance-dependent slope for the diffuse emission in the TeV range are rather different, as highlighted by Lipari & Vernetto (2018), Cataldo et al. (2019). In the universal cosmic-ray spectrum model, the softer spectrum of the outer Galaxy and high Galactic latitude emission could in principle be explained by the influence of individual local cosmic-ray sources, which contribute sizeably to the cosmic-ray population around the Sun (Kachelrieß et al. 2015, 2018a; Bouyahiaoui et al. 2019) and distort the spectrum of diffuse emission in a limited energy range and in a limited sky region. In contrast, in the model of distance-dependent cosmic-ray spectrum, the propagation regime of cosmic rays through the interstellar medium changes because the structure of the turbulent Galactic magnetic fields changes systematically. This determines the energy-dependent diffusion of cosmic rays.

The potential of the highest energy measurements of the sky emission by the LAT has been explored by Neronov et al. (2018), who reported the first measurement of the large-scale diffuse flux of the TeV sky. This measurement used the `P8R2_ULTRACLEANVETO_V6` event selection of LAT events, which was characterised by the lowest residual cosmic-ray background, when it was considered as a direct implementation to a similar Pass 7 event selection (Ackermann et al. 2015). However, no detailed information on the residual cosmic-ray background level in `P8R2_ULTRACLEANVETO_V6` was available. Knowledge of the level of residual cosmic-ray background is important for studying diffuse TeV emission because in this energy range the cosmic-ray background starts to contribute significantly to the event sample.

The *Fermi*/LAT collaboration has recently released the new photon selection `P8R3_SOURCEVETO_V2` (Bruel et al. 2018), which provides the suppression of the charged cosmic-ray background comparable to that of the `ULTRACLEANVETO` class, but has larger event statistics, comparable to `P8R2_CLEAN_V6` (Bruel et al. 2018; Ackermann et al. 2018). Motivated by this improvement, we performed a more advanced analysis of the hard TeV diffuse emission, which we report below. The higher signal statistics and lower level of residual cosmic-ray background enable studying the spatial morphology of the signal and better characterising its spectral properties. The better data quality enables a direct comparison with the ground-based γ-ray telescope measurements. We perform this comparison in the following sections. We also recalculate the properties of the high Galactic latitude diffuse emission, after characterising the residual cosmic-ray background in the `P8R3_SOURCEVETO_V2` event selection.

2. Data analysis

2.1. Fermi/LAT

Our analysis is based on *Fermi*/LAT data that were collected within the time interval 2008 October 27 to 2019 June 20 (we excluded the first month of *Fermi*/LAT operations when the veto was not operating properly[1]). We filtered the data to retain only events belonging to the `P8R3_SOURCEVETO_V2` class (Bruel et al. 2018), which has the best quality of the residual cosmic-ray background rejection. We processed the LAT event list using the *gtselect-gtmktime* chain to remove photons `zmax = 100` and `(DATA_QUAL>0)&&(LAT_CONFIG==1)` following the recommendations of the *Fermi*/LAT team[2].

Next, we divided the γ-ray event set into two parts: one for the diffuse emission components and another for the resolved sources listed in the 4FGL catalogue (Acero et al. 2015). To do this, we collected photons within circles of radius 0.5° around the 4FGL sources and estimated the level of diffuse background within these circles by counting the number of photons per steradian in the parts of the sky outside the 0.5° circles. We then calculated the cumulative 4FGL source flux within the 0.5° circles by subtracting the estimated background from the photon counts. Finally, we estimated the total 4FGL source flux by correcting for the fraction of the signal contained within the 0.5° radius as a function of energy. We estimated this fraction based on the radial profiles of the photon distribution around bright sources Crab, Geminga, and Mrk 421.

To calculate the spectra of cumulative point source flux and diffuse fluxes in different parts of the sky, we calculated the exposure using the *gtexpcube2* routine for the exposure map in 14 logarithmically equally spaced energy bins between 1 GeV and 3.16 TeV (the highest energy to which the LAT response is calculated).

2.2. Estimating the residual cosmic-ray background

The level of photon fluxes that we aim to explore is so low that the contribution of the residual cosmic-ray background into the signal could possibly not be neglected. With this in mind, we used the methods developed by Ackermann et al. (2015), Bruel et al. (2018), Neronov & Semikoz (2012a) to extract an estimate of the level of residual cosmic-ray background in the `SOURCEVETO` event selection as a function of energy.

We first estimated the contamination of the `SOURCEVETO` events by the residual cosmic rays in three energy bins for which the information is implicitly given by Bruel et al. (2018): 25–40 GeV, 80–125 GeV, and 250–400 GeV. Bruel et al. (2018) list the residual cosmic-ray fraction for the `SOURCE` class events for the high-latitude diffuse (HLD) sky region, which corresponds to the Galactic latitude $|b| > 20°$, excluding circles of radius 0.2° around 3GFL sources[3] and excluding the region occupied by the *Fermi* bubbles, which we assumed to be within the Galactic longitude $-45° < l < 45°$. We used the same sky region in our analysis. The HLD event statistics is compared to that of reference (REF) pure gamma events collected from circles of radius 0.2° around 3GFL sources at Galactic latitudes $|b| > 20°$, in the central Galaxy

[1] https://fermi.gsfc.nasa.gov/ssc/data/analysis/LAT_caveats.html

[2] https://fermi.gsfc.nasa.gov/ssc/data/analysis/

[3] We used the third version of the *Fermi*/LAT catalogue in the residual cosmic-ray fraction analysis to be consistent with analysis of Bruel et al. (2018), but we use the current 4FGL catalogue in the original analysis in the following sections.

Table 1. Fraction of residual cosmic-ray background events in the SOURCE class in three reference energy bins, estimated based on Bruel et al. (2018).

Energy (GeV)	α	β
25–40	0.16 ± 0.008	0.95 ± 0.02
80–125	0.29 ± 0.02	0.93 ± 0.05
250–400	0.59 ± 0.05	0.90 ± 0.12

region at $|l| < 90°, |b| < 5°$, and from the Earth limb in a zenith angle range $111° < Zd < 113°$. We provide a detailed demonstration of the very low contamination of the REF event sample by residual cosmic-ray background in Appendix A.

Bruel et al. (2018) have calculated the signal in the anti-coincidence detector of the LAT ($S_{\rm tile}$) for REF and all HLD events belonging to the SOURCE class. We used these results to determine the total number of all HLD events, $N_{\rm HLD,S}$, and REF events, $N_{\rm REF,S}$, and also their difference, $N_{\rm CR,S} = N_{\rm HLD,S} - N_{\rm REF,S}$. This enables estimating the residual cosmic-ray fraction in the SOURCE event selection in the HLD region,

$$\alpha = \frac{N_{\rm CR,S}}{N_{\rm HLD,S}}. \quad (1)$$

The values of α for the three energy bins are given in Table 1.

Knowing the number of residual cosmic-ray events $N_{\rm CR,S}$ in the SOURCE class event selection, we calculated the number of residual cosmic-ray events in the SOURCEVETO selection in the same HLD region, $N_{\rm CR,SV}$, using the method of Neronov & Semikoz (2012a). Following this approach, we first compared the statistics of events $N_{\rm REF,S}$, $N_{\rm REF,SV}$ of the SOURCE and SOURCEVETO classes in the REF samples, that is, the pure photon events in each event class. The resulting ratio

$$\beta = \frac{N_{\rm REF,SV}}{N_{\rm REF,S}} \quad (2)$$

is given in the third column of Table 1. The measurement of β has allowed us to calculate the number of photon events in the HLD photon sample for the SOURCEVETO class,

$$N_{\gamma,\rm SV} = \beta N_{\gamma,\rm S} = \beta(1-\alpha) N_{\rm HLD,S}. \quad (3)$$

Finally, we estimated the number of residual cosmic-ray events in the SOURCEVETO event sample in the HLD region by subtracting the photon event counts from the total event counts in the HLD region,

$$N_{\rm CR,SV} = N_{\rm HLD,SV} - N_{\gamma,\rm SV}. \quad (4)$$

Measurements of $N_{\rm CR,SV}$ in the three energy bins of Bruel et al. (2018) are shown in Fig. 1 by the red data points.

To estimate the residual cosmic-ray background at energies different from those of the three energy bins discussed by Bruel et al. (2018), we used the results of Ackermann et al. (2015) on the residual cosmic-ray background rate spectrum, $dN_{\rm CR}(E)/dE$, which is a power-law function of the energy in the energy range of interest (it is the rate, rather than physical flux, which is a power law in energy). This assumption is consistent with the measurement of $N_{\rm CR,SV}$ for the three reference energies derived above, as Fig. 1 shows. We added one more data point in the energy range 3–10 TeV by assuming that the totality of the counts in the HLD region at this energy belongs to the residual cosmic-ray background (there are three events in the sample).

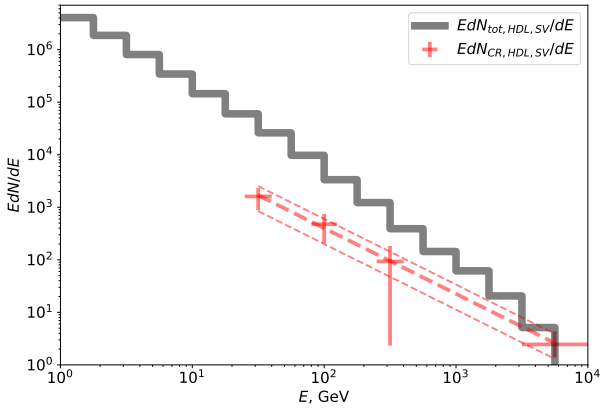

Fig. 1. Residual cosmic-ray background counts $dN_{\rm CR,HLD,SV}/dE$ in the HLD region for the SOURCEVETO event selection (red data points and power-law fit) compared to the total counts $dN_{\rm HLD,SV}/dE$ as a function of energy (grey histogram).

If this is not the case, the total count statistics in this energy bin provides at least an upper limit on $N_{\rm CR,SV}$ in this energy range.

Fitting the power-law model to the measurements at the four energies, we find the differential count rate spectrum $dN_{\rm CR,SV}(E)/dE$. The residual cosmic-ray background contamination of the event sample could be expressed in terms of an equivalent isotropic sky flux, if the event counts are divided by the γ-ray exposure (expressed in cm^2 s) for the HLD sky region, even though the cosmic rays, strictly speaking, do not constitute part of the flux from the sky. In this representation, the residual cosmic-ray background level is shown in Fig. 5. As a cross-check of the correctness of our estimate of the residual cosmic-ray background, we show in the same figure the calculation of the isotropic background template for the P8R3_SOURCEVETO_V2 event selection calculated by Bruel et al. (2018). The isotropic background includes both the isotropic γ-ray background (IGRB) derived by Ackermann et al. (2015) and the residual cosmic-ray background. Below an energy of 300 GeV, the isotropic background is dominated by the IGRB contribution. Above this energy, the residual cosmic-ray background dominates. The estimate of the isotropic background by Bruel et al. (2018) is within the uncertainty range of our estimate of the residual cosmic-ray background in this energy range.

3. Results

3.1. TeV diffuse emission from the Galactic plane

The strongest TeV signal comes from the Galactic plane, which contributes about 60% of the all-sky signal.

The Galactic longitude profile of the signal is shown in Fig. 2. The signal is collected in bins spanning $10° \times 10°$ within a $|b| < 2°$ strip around the Galactic plane in the energy range from 0.5 TeV to 2 TeV. The signal is detected above the residual cosmic-ray background level (the equivalent flux is 10^{-11}/(TeV cm^2 s sr)) at all Galactic longitudes. Emission from 4FGL sources dominates the overall Galactic plane flux within $|l| < 50°$ of the inner Galactic plane part, the diffuse emission provides the dominant flux component in the outer Galaxy.

Detection of the diffuse Galactic plane signal at TeV has previously been reported by the HESS (Abramowski et al. 2014) and ARGO-YBJ (Bartoli 2015) collaborations. Figures 3 and 4 provide a comparison of *Fermi*/LAT measurements with these previous measurements.

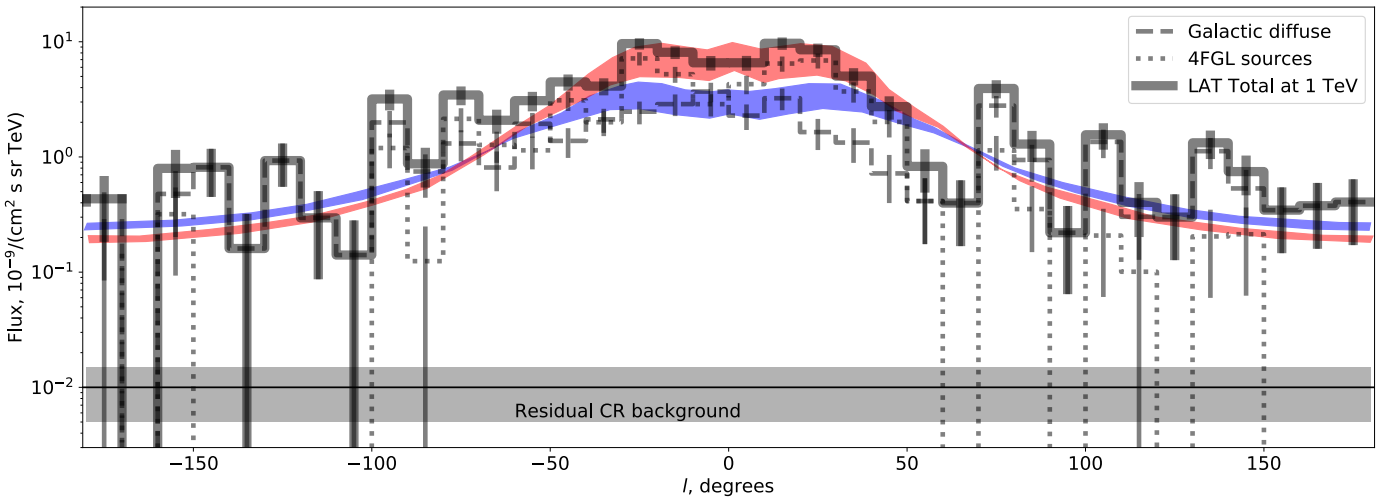

Fig. 2. Galactic longitude profile of the signal from Galactic latitude range $|b| < 2°$. Dashed and dotted lines show the diffuse and resolved 4FGL source flux components. Solid line is the sum of the two components. Blue and red model curves are from Cataldo et al. (2019). Grey band shows the level of residual cosmic ray background.

There is a significant difference between the measurements of *Fermi*/LAT and HESS (which should be considered as a lower bound on the flux; Abramowski et al. 2014). The overall (resolved source + diffuse emission) flux measured by HESS in the $-80° < l < 60°$ part of the Galactic Plane within the Galactic latitude range $|b| < 2°$ is almost everywhere lower than the *Fermi*/LAT measurements of the flux from the same sky region. The only exception is the region $30° < l < 60°$, where the two flux measurements are compatible.

The agreement between *Fermi*/LAT and ARGO-YBJ (Bartoli 2015) measurement of the flux within the $|b| < 5°$ strip is better. The two measurements are consistent in large parts of the Galactic plane, except for the Cygnus region at $l \sim 80°$, where the LAT detects much higher flux and in the outer Galaxy part of the Galactic plane, $140° < l < 170°$, where ARGO-YBJ does not detect any diffuse emission flux, while *Fermi*/LAT has significant flux detection.

The separation of the total flux into diffuse and resolved source components strongly depends on (a) the number of resolved sources in each telescope and (b) the angular cut on the source extent for the extended sources. Most of the sources in the inner Galactic plane are extended, and the extensions measured by HESS are different from those measured by *Fermi*/LAT (Neronov & Semikoz 2012b). Because of this fact, a stronger discrepancy is noted between the *Fermi*/LAT and HESS measurements of the diffuse emission component. The diffuse emission flux measured by the LAT has a level that is comparable to the total flux measured by HESS, while the HESS estimate of the diffuse emission is almost an order of magnitude lower.

We attribute the discrepancies between the *Fermi*/LAT and HESS measurements to the peculiarity of the background subtraction in the HESS data. First, the HESS source detection method relies on the ring background estimate method in which the background level is judged based on the count statistics in ring segments around the reference point at which the γ-ray signal is estimated. This assumes that there is no γ-ray emission at the background ring position, which is not correct in the case of the signal of the Galactic plane.

Next, the HESS analysis of the diffuse emission assumed that there is no diffuse emission signal outside the $|b| < 1.5°$ strip. Figure 4 shows that this is not the case. The Galactic latitude profile of the HESS signal has to converge to zero by construction at $|b| = 1.5°$. The *Fermi*/LAT analysis does not rely on the assumption of the absence of the signal at $|b| > 1.5°$, and indeed, the signal is not zero in this region. The signal that is measured by *Fermi*/LAT at $|b| > 1.5°$ is counted as part of the background in the HES analysis. This leads to an over-estimate of the background level. The difference between the *Fermi*/LAT measurements and the HESS lower bounds is more sophisticated in the Galactic longitude profiles, but the origin of the difference remains the same. The over-estimate of the background in the HESS measurements depends on the Galactic longitude, so that the discrepancy between *Fermi*/LAT and HESS also depends on the Galactic longitude. This explanation of the discrepancy between the *Fermi*/LAT and HESS profiles is supported by the fact that the level of diffuse flux measured by *Fermi*/LAT in the HESS background estimate regions is comparable to the overall mismatch between the *Fermi*/LAT and HESS diffuse flux measurements within the ±2° strip around the Galactic plane.

The ARGO-YBJ background estimate method is different and by construction less sensitive to the details of the γ-ray signal distribution in the immediate vicinity of the Galactic lane. ARGO-YBJ estimates the background in strips of constant declination, which mostly contain regions of high Galactic latitude, where the γ-ray flux level decreases significantly.

The TeV γ-ray signal for the Galactic plane provides information on the distribution of cosmic rays with energies $E > 10$ TeV in the Galaxy (Neronov & Malyshev 2015; Yang et al. 2016; Acero et al. 2016). Uncertainties in the cosmic-ray source distribution throughout the Galactic disc and uncertainties in the details of cosmi-ray diffusion out of the disc lead to large uncertainties in modelling the diffuse emission flux throughout the Galactic plane. This is illustrated in Fig. 2, where recent models of the TeV Galactic plane emission calculated by Cataldo et al. (2019) are shown. The level of diffuse emission is approximately reproduced in the inner Galactic plane by a model that assumes that the cosmic-ray spectral slope is harder than the locally observed slope in the inner Galaxy. However, as we discussed above, the separation of the total emission into diffuse and source components strongly depends on the assumptions about the nature and morphology of the detected sources. A large part of the detected sources might be tracing the

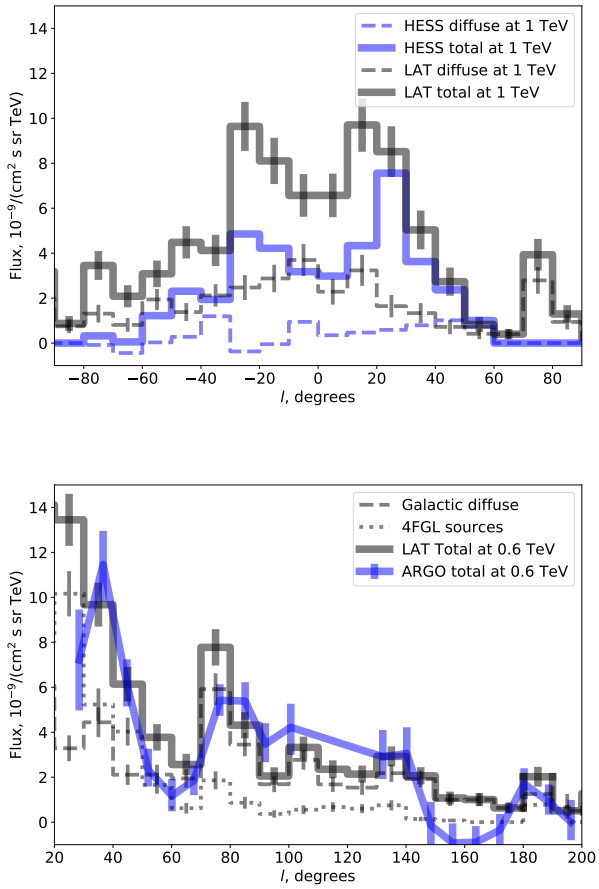

Fig. 3. *Top*: *Fermi*/LAT (black) and HESS (blue) measurements of the Galactic plane flux at 1 TeV energy within a strip $|b| < 2°$. *Bottom*: *Fermi*/LAT (black) and ARGO-YBJ (blue) measurements of the Galactic plane flux within the $|b| < 5°$ strip in the energy range around 0.6 TeV. Notations are the same as in Fig. 2. Dashed lines show diffuse emission, and solid lines are the total flux (diffuse emission plus resolved sources).

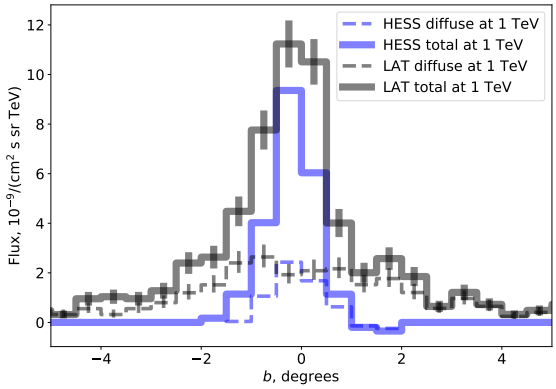

Fig. 4. *Fermi*/LAT and HESS measurements of the Galactic latitude profile of the inner Galactic plane strip $-80° < l < 60°$. Notations are the same as in Fig. 3.

injection points of cosmic rays (Neronov & Semikoz 2012b), and in this respect, they should be considered as part of the emission from cosmic-ray interactions. In this case, the model with the distance-independent cosmic-ray injection spectrum traces the TeV flux better.

Models with a distance-dependent and a universal cosmic-ray spectrum in the Galactic disc also predict different shapes

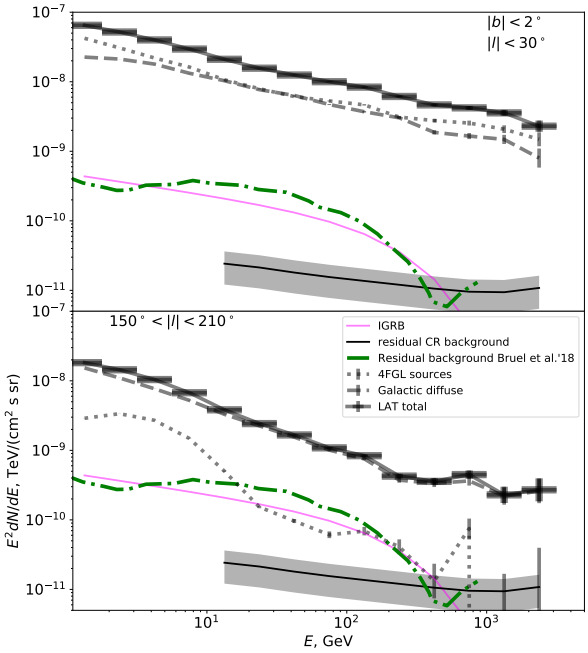

Fig. 5. Emission spectrum from the low Galactic latitude region $|b| < 10°$. *Top and bottom panels* refer to the inner, $|l| < 30°$, and outer, $150° < l < 210°$, Galaxy segments. Dashed and dotted lines show the diffuse background and resolved 4FGL source components of the flux. Solid lines show the sum of the two components. The thin solid magenta line shows the IGRB reported by Ackermann et al. (2015). For comparison, the spectrum of the isotropic background template for the `P8R3_SOURCEVETO_V2` event selection, calculated by Bruel et al. (2018), is shown by the green dash-dotted line. This isotropic background template includes the IGRB and the residual cosmic-ray background components.

of the spectrum in different directions along the disc (Lipari & Vernetto 2018). Figure 5 shows a comparison of the spectra of diffuse emission from the Galactic ridge ($|l| < 30°$) and the outer Galactic plane ($150° < l < 210°$). In the energy range between 30 and 300 GeV, the two spectra clearly have different slopes. This could be well explained by the phenomenological model of the Galactic distance-dependent slope of the average cosmic-ray spectrum (Gaggero et al. 2015), and also by the model of the universal hard cosmic-ray spectrum, with the effect of the local source imprinted on the outer Galaxy spectrum (Neronov & Malyshev 2015; Kachelrieß et al. 2018a; Bouyahiaoui et al. 2019). However, the TeV band spectra of the two regions have consistent slopes: $\Gamma = 2.38 \pm 0.12$ for the Galactic ridge, and $\Gamma = 2.23 \pm 0.16$ for the outer Galactic plane. This is difficult to explain in the model of Gaggero et al. (2015), in which the outer Galactic disc spectrum has to remain soft in the TeV range as well.

The hard spectrum of the outer Galactic disc is consistent with the model of anisotropic cosmic-ray diffusion, which reconciles the measurement of the structure of the Galactic magnetic field and cosmic-ray data (Giacinti et al. 2018). Within this model, a small number of cosmic-ray sources provides a sizeable fractional contribution to the overall local cosmic-ray population and to the local γ-ray emissivity of the interstellar medium (Kachelrieß et al. 2018a; Bouyahiaoui et al. 2019). In contrast, due to the projection effects, many more sources contribute to the spectrum of the Galactic disc, so that its slope provides a measurement of the average slope of the Galactic cosmic-ray population (Neronov & Malyshev 2015).

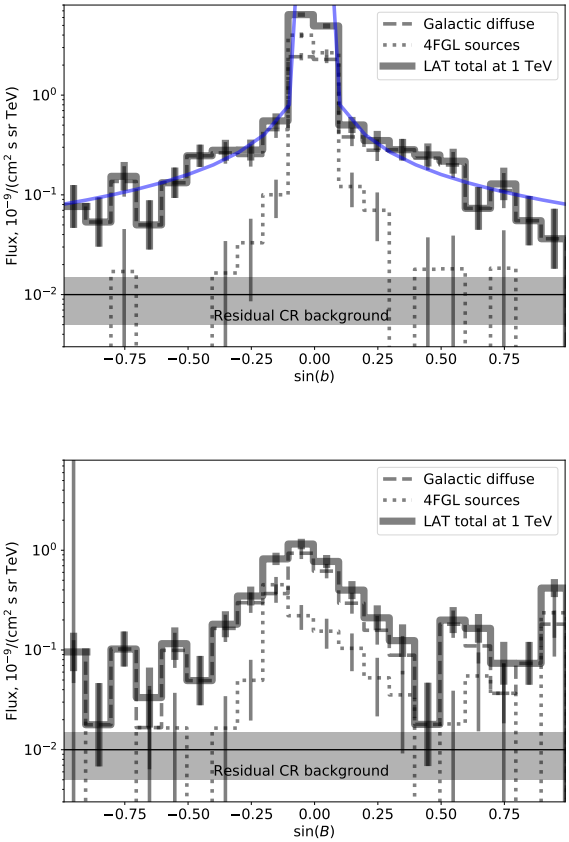

Fig. 6. Galactic latitude profiles of the inner Galactic plane strips $-60° < l < 60°$ (*top panel*) and $120° < l < 240°$ (*bottom panel*). The blue curve shows the emission from a disc with constant thickness. The other notations are the same as in Fig. 2.

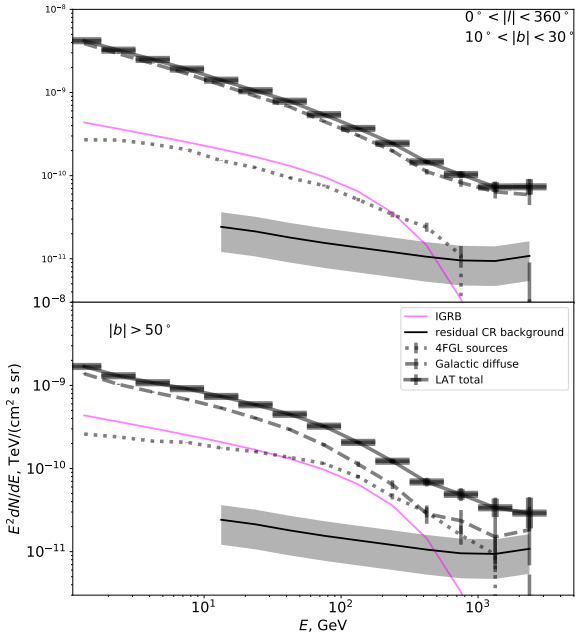

Fig. 7. Spectra of high Galactic latitude regions: mid-latitudes $10° < |b| < 30°$ (*top panel*) and the Galactic pole regions $|b| > 50°$ (*bottom panel*). The notations are the same as in Fig. 5.

3.2. High Galactic latitude emission

Although the level of diffuse Galactic emission outside the Galactic plane is much lower, its flux is still detected at a high significance level. Figure 6 shows the Galactic latitude profile of the signal from the same strip as in Fig. 4, but up to the high Galactic latitude range (binned linearly in sin(b)). The emission is detected in the Galactic pole regions (the highest latitude bins span $65° < |b| < 90°$), well above the residual cosmic-ray background level. The high Galactic latitude profile is consistent with the simple model of emission from a homogeneous disc of constant thickness. In this model the signal is proportional to the column density of the disc, which scales as $1/\sin|b|$ with Galactic latitude. This model is shown by the blue line in the top panel of Fig. 6.

The simple constant-thickness disc model does not fit the profile of the TeV signal in the outer Galaxy direction in the sector $120° < l < 240°$, as the bottom panel of Fig. 6 shows. The central part of the disc emission at low latitude is missing and the signal has high-latitude flattening. This is perhaps explained by the truncation of the Galactic disc beyond the solar radius and/or by the presence of the complex local interstellar medium, with the Local Bubble (Frisch et al. 2011) introducing large variations in the column density of the interstellar material in different directions.

The high Galactic latitude signal contains a resolved source and diffuse components. The spectra of the two components in the TeV range are significantly different, as shown in Fig. 7. The flux of the resolved source component is soft and sub-dominant, compared to the diffuse emission. The resolved source flux (dominated by distant active galactic nuclei) does not depend on Galactic latitude. Its spectral shape approximately repeats that of the IGRB (Neronov & Semikoz 2012a; Ackermann et al. 2015).

In contrast, the diffuse emission level depends on the Galactic latitude. It is interesting to note that the slopes of the 0.3–3 TeV diffuse emission spectrum at different Galactic latitudes are consistent with the slope of the Galactic plane. In the latitude range $|b| > 50°$, the slope measurement is $\Gamma = 2.39 \pm 0.13$, and in the $10° < |b| < 30°$ region, it is $\Gamma = 2.43 \pm 0.06$. Combining the measurements of the 0.3–3 TeV spectral slopes in four different parts of the sky (inner and outer Galactic plane, the Galactic poles, and the mid-latitude regions), we find an average slope $\Gamma = 2.40 \pm 0.05$ with which the spectra of all the four regions are consistent.

4. Discussion

The new *Fermi*/LAT event selection `P8R3_SOURCEVETO_V2` is characterised by a very low level of residual cosmic-ray background and by relatively high statistics of the γ-ray signal in the TeV energy range. These properties of the data have allowed us to study the properties of TeV Galactic diffuse emission from different parts of the sky.

Surprisingly, the overall level of the TeV γ-ray flux from the inner Galactic plane detected by *Fermi*/LAT is approximately twice higher than the flux detected by the HESS telescope from the analysis of the Galactic plane survey region (Abramowski et al. 2014). We attribute this discrepancy to the subtleties of the background estimate in the ground-based Cherenkov telescopes. Cherenkov telescopes have narrow fields of view, which complicates the task of mapping the diffuse emission on large angular scales.

The comparison of *Fermi*/LAT and HESS measurements provides an indication of how the ground-based measurements can be improved. The measurement quality of diffuse Galactic plane emission with ground-based instruments will be

significantly improved with the start of operation of small-size telescopes of the Cherenkov Telescope Array (CTA; Actis et al. 2011), which will have a much wider field of view than HESS. This will enable a more reliable estimate of the background from higher Galactic latitude regions using the ring background technique. Still, thee γ-ray flux measurement will be significantly contaminated by the cosmic-ray and incorrectly attributed γ-ray background flux even if the Galactic latitude range of the background regions is extended up to $|b| \sim 5^\circ$. Perhaps the best background modelling technique for the CTA is to rely on *Fermi*/LAT measurements in the energy range of interest and use an imaging template found from *Fermi*/LAT data in the analysis of individual point and extended sources.

Our analysis shows that diffuse emission spectrum is hard in different parts of the sky, as first noted by Neronov et al. (2018), based on the analysis of `ULTRACLEANVETO` Pass 7 event selection with custom cross-calibration of *Fermi*/LAT with ground-based telescope measurements. We have used higher statistics of the TeV band signal and better calibrations available in the `P8R3_SOURCEVETO_V2` event selection for a more detailed investigation of the spectral and imaging properties of the hard emission. Additionally, we were able to quantify the residual cosmic-ray background contamination of the `P8R3_SOURCEVETO_V2` signal and to verify that the hard spectral component is not generated by this contamination.

The slope $\Gamma = 2.40 \pm 0.05$ of the TeV diffuse emission in different parts of the sky is harder than that of the locally measured cosmic-ray spectrum, which changes from $\Gamma > 2.8$ in the energy range below 200 GeV (Aguilar et al. 2015; Adriani et al. 2011) to $\Gamma \sim 2.6$ in the multi-TeV range (Yoon et al. 2017; Gorbunov et al. 2018) (see Kachelrieß & Semikoz 2019 for a recent review). It is, however, consistent with slope of the average Galactic cosmic-ray spectrum in the inner Galaxy measured based on a study of the lower energy γ-ray diffuse emission (Neronov & Malyshev 2015; Yang et al. 2016; Acero et al. 2016). It is surprising that this hard slope is also found in high Galactic latitude and outer Galactic disc regions. In addition to the possibility that the TeV diffuse emission spectral slope corresponds to the slope of the average Galactic cosmic-ray population, possible models of the hard TeV component include diffuse emission from the interstellar medium of the local Galaxy produced by cosmic rays that spread from a nearby source into a (local) super-bubble (Andersen et al. 2018; Bouyahiaoui et al. 2019), or emission from the large (100 kpc scale) cosmic-ray halo around the Milky Way (Taylor et al. 2014) or decays of super-heavy dark matter particles (Esmaili & Serpico 2013; Murase et al. 2015; Kachelrieß et al. 2018b).

It was noted by Neronov et al. (2014, 2018), Neronov & Semikoz (2016a,b) that the flux level and spectral properties of the hard diffuse multi-TeV high Galactic latitude emission detected by *Fermi*/LAT are compatible with those of the IceCube neutrino signal from different parts of the sky either in the high-energy starting or muon neutrino channel at much higher energies $E > 100$ TeV. In this sense, the hard spectrum 0.3–3 TeV Galactic diffuse emission could be the γ-ray counterpart of the high Galactic latitude neutrino flux. Before this nature of the multi-TeV γ-ray signal can be firmly established, it is important to extend the measurements into the energy band that reaches the IceCube energy range (10 TeV). This is possible, in principle, because the LAT detects photons with energies up to 10 TeV. The Galactic plane signal is clearly identifiable in the sky map between 3 and 10 TeV. However, the instrument characteristics of the LAT are not known because of the absence of Monte Carlo modelling of the instrument response similar to that reported by Bruel et al. (2018). This modelling has also to include the modelling of the residual cosmic-ray background that contaminates the signal more strongly in this energy range. Further improvement of the statistics of the space-based measurements of diffuse emission in the multi-TeV band should be possible with a larger space-based γ-ray telescope, such as High Energy Radiation Detector (HERD; Zhang et al. 2014).

A complementary probe of the hard component of Galactic γ-ray flux in the multi-TeV band is also possible with a dedicated ground-based γ-ray detector providing sufficiently strong suppression of the charged cosmic-ray background. This could be achieved by measuring the muon content of extensive air showers, through observations with Cherenkov telescopes at large zenith angle (Neronov et al. 2016), or using underground muon detectors, as demonstrated by the KArlsruhe Shower Core and Array DEtector (KASCADE) experiment (Apel et al. 2017) and as planned in the Carpet-3 detector (Dzhappuev et al. 2019).

References

Abdo, A. A., Allen, B., Aune, T., et al. 2008, ApJ, 688, 1078
Abramowski, A., Aharonian, F., Ait Benkhali, F., et al. 2014, Phys. Rev. D, 90, 122007
Acero, F., Ackermann, M., Ajello, M., et al. 2015, ApJS, 218, 23
Acero, F., Ackermann, M., Ajello, M., et al. 2016, ApJS, 223, 26
Ackermann, M., Ajello, M., Albert, A., et al. 2015, ApJ, 799, 86
Ackermann, M., Ajello, M., Baldini, L., et al. 2018, Phys. Rev. Lett., 121, 241101
Actis, M., Agnetta, G., Aharonian, F., et al. 2011, Exp. Astron., 32, 193
Adriani, O., Barbarino, G. C., Bazilevskaya, G. A., et al. 2011, Science, 332, 69
Aguilar, M., Aisa, D., Alpat, B., et al. 2015, Phys. Rev. Lett., 114, 171103
Andersen, K. J., Kachelriess, M., & Semikoz, D. V. 2018, ApJ, 861, L19
Apel, W. D., Arteaga-Velázquez, J. C., Bekk, K., et al. 2017, ApJ, 848, 1
Atwood, W. B., Abdo, A. A., Ackermann, M., et al. 2009, ApJ, 697, 1071
Bartoli, B., Bernardini, P., Bi, X. J., et al. 2015, ApJ, 806, 20
Bouyahiaoui, M., Kachelriess, M., & Semikoz, D. V. 2019, JCAP, 1901, 046
Bruel, P., Burnett, T. H., Digel, S. W., et al. 2018, ArXiv e-prints [arXiv:1810.11394]
Cataldo, M., Pagliaroli, G., Vecchiotti, V., & Villante, F. L. 2019, J. Cosmol. Astropart. Phys., 12, 050
Dzhappuev, D. D., Dzaparova, I. M., Gorbacheva, E. A., et al. 2019, EPJ Web Conf., 207, 03004
Esmaili, A., & Serpico, P. D. 2013, JCAP, 11, 054
Frisch, P. C., Redfield, S., & Slavin, J. D. 2011, ARA&A, 49, 237
Gaggero, D., Urbano, A., Valli, M., & Ullio, P. 2015, Phys. Rev. D, 91, 083012
Giacinti, G., Kachelriess, M., & Semikoz, D. V. 2018, JCAP, 1807, 051
Gorbunov, N., Grebenyuk, V., Karmanov, D., et al. 2018, ArXiv e-prints [arXiv:1809.05333]
Kachelrieß, M., Neronov, A., & Semikoz, D. V. 2015, Phys. Rev. Lett., 115, 181103
Kachelrieß, M., Neronov, A., & Semikoz, D. V. 2018a, Phys. Rev. D, 97, 063011
Kachelrieß, M., Kalashev, O. E., & Kuznetsov, M. Yu. 2018b, Phys. Rev. D, 98, 083016
Kachelrieß, M., & Semikoz, D. V. 2019, Prog. Part. Nucl. Phys., 109, 103710
Lipari, P., & Vernetto, S. 2018, Phys. Rev. D, 98, 043003
Murase, K., Laha, R., Ando, S., & Ahlers, M. 2015, Phys. Rev. Lett., 115, 071301
Neronov, A., & Semikoz, D. V. 2012a, ApJ, 757, 61
Neronov, A., & Semikoz, D. V. 2012b, Phys. Rev. D, 85, 083008
Neronov, A., Semikoz, D., & Tchernin, C. 2014, Phys. Rev. D, 89, 103002
Neronov, A., & Malyshev, D. 2015, ArXiv e-prints [arXiv:1505.07601]
Neronov, A., & Semikoz, D. 2016a, Astropart. Phys., 72, 32
Neronov, A., & Semikoz, D. 2016b, Astropart. Phys., 75, 60
Neronov, A., Semikoz, D. V., Vovk, I., & Mirzoyan, R. 2016, Phys. Rev. D, 94, 123018
Neronov, A., Kachelrieß, M., & Semikoz, D. V. 2018, Phys. Rev. D, 98, 023004
Taylor, A. M., Gabici, S., & Aharonian, F. 2014, Phys. Rev. D, 89, 103003
Yang, R., Aharonian, F., & Evoli, C. 2016, Phys. Rev. D, 93, 123007
Yoon, Y. S., Anderson, T., Barrau, A., et al. 2017, ApJ, 839, 5
Zhang, S. N., Adriani, O., Albergo, S., et al. 2014, in Space Telescopes and Instrumentation 2014: Ultraviolet to Gamma Ray, SPIE Conf. Ser., 9144, 91440X

Appendix A: Residual cosmic-ray background contamination of the REF event sample

The REF event sample introduced by Bruel et al. (2018) is almost exclusively composed of γ-ray events in the three energy bins considered in the analysis reported by Bruel et al. (2018). An upper limit on the residual cosmic-ray contamination of this sample could be readily derived from a comparison of the statistics of REF events with that of events from the sky region that might have the highest contamination by the residual cosmic rays: the Galactic poles at $|b| > 80°$.

This comparison is given in Table A.1. In this table, the statistics of different contributions to the REF sample is summarised. $N_{\rm source}$ denotes the events within the 0.2° circles around the 3FGL sources at Galactic latitudes $|b| > 20°$, $N_{\rm Gal}$ is the number of events from the inner Galactic disc $|l| < 90°$, $|b| < 5°$, and $N_{\rm limb}$ is the number of events from the direction of the Earth limb at zenith angles $111° < Zd < 113°$.

We derive an upper limit on the number of residual cosmic-ray events in the REF sample, $N_{\rm CR}$, from the event statistics in the north and south Galactic poles at $|b| > 80°$, which is shown in Table A.2. The total event counts in these regions, $N_{\rm tot}$, have four contributions: the resolved point source counts $N_{\rm source}$, the isotropic γ-ray background $N_{\rm igrb}$, the Galactic diffuse emission $N_{\rm diff}$, and the residual cosmic-ray background $N_{\rm CR,poles}$. We calculated $N_{\rm source}$ by collecting photons from the circles of 0.2° around known catalogue sources and correcting for the energy-dependent fraction of the point source flux contained within the 0.2° circles. Subtracting $N_{\rm source}$ from the total counts, we find

$$N_{\rm CR,poles} < N_{\rm CR,poles} + N_{\rm IGRB} + N_{\rm diff} = N_{\rm tot} - N_{\rm source}. \quad (A.1)$$

In this way we obtain a robust upper limit on $N_{\rm CR,poles}$, rather than measurement, but this is sufficient for the demonstration of low contamination of the REF event sample by the residual cosmic rays.

After determining an upper limit on $N_{\rm CR,poles}$, we derived from it an upper limit on the number of residual cosmic-ray events in the REF event selection by rescaling the $N_{\rm CR,poles}$ upper limit considering the difference in solid angle from which the signals from the Galactic poles and REF regions are collected. The regions at $|b| > 80°$ span the solid angle $\Omega_{|b|>80°} \simeq 0.19$ sr. The regions of which the REF sample is composed span overall a solid angle $\Omega_{\rm REF} \simeq 0.82$ sr. Thus, the number of cosmic-ray events in the REF sample is

$$N_{\rm CR} = \frac{\Omega_{\rm REF}}{\Omega_{|b|>80°}} N_{\rm CR,poles} < \frac{\Omega_{\rm REF}}{\Omega_{|b|>80°}} (N_{\rm tot} - N_{\rm source}). \quad (A.2)$$

This upper bound is given in Table A.1.

We include this upper bound as the systematic error on the measurement of the number of γ-rays in the REF regions and add it in quadrature to the statistical uncertainty of $N_{\rm REF}$, as specified in the last column of Table A.1. This uncertainty is then included in the calculation of the uncertainty of α reported in Table 1.

Table A.1. Statistics of events in the REF event sample of Bruel et al. (2018).

Energy (GeV)	$N_{\rm source}$	$N_{\rm Gal}$	$N_{\rm limb}$	$N_{\rm REF}$	$\sqrt{N_{\rm REF}}$	$N_{\rm CR}$	$\sqrt{N_{\rm REF} + N_{\rm CR}^2}/N_{\rm REF}$
25–40	5524	47 406	227 668	280 598	530	<2071	0.8%
80–125	958	8641	31 626	41 225	203	<397	1.1%
250–400	136	1744	4968	6848	83	<95	1.8%

Table A.2. Statistics of events in the north and south Galactic poles.

Energy (GeV)	$N_{\rm tot}$	$N_{\rm 3GFL}$	$N_{\rm diff} + N_{\rm IGRB} + N_{\rm CR,poles}$
25–40	784	304	480
80–125	154	62	92
250–400	33	11	22